Proceedings of the 28th IEEE
EMBS Annual International Conference
New York City, USA, Aug 30-Sept 3, 2006

Nonlinear analysis of heart murmurs using wavelet-based higher-order spectral parameters

Styliani A. Taplidou, *Student Member, IEEE* and Leontios J. Hadjileontiadis, *Member, IEEE*

***Abstract*—The aim of this study was to reveal and analyze the nonlinear characteristics of heart sounds, reflected in the quadrature phase coupling of the contained frequencies, as they evolve over time. To achieve this, the continuous wavelet transform was combined with third-order statistics/spectra in order to analyze their non Gaussian character, taking into account their non-stationarity. Heart sounds from patients with several pathologies that exhibit murmurs were drawn from a heart sound database and analyzed in the time-bi-frequency domain. The analysis results justified the efficient performance of this combinatory approach to reveal and quantify the evolution of heart murmurs nonlinearities with time.**

I. Introduction

THE DIAGNOSTIC value of heart sounds has been known since the years of Hippocrates. Cardiac auscultation constitutes until nowadays a non-invasive and inexpensive diagnostic method. During the last decades, the evolution of computers and their introduction in clinical practice has led to new signal analysis techniques, which reveal heart sound characteristics that are related to several pathologies [1]-[6].

There are two main heart sounds that are normally present, S1 and S2. The heart sound S1 is associated with the closure of the mitral and tricuspid valves, whereas S2 is the result of the closure of the aortic and pulmonic valves. Apart from S1 and S2, other sounds can also be heard, such as heart murmurs. Murmurs are defined as sustained noises that are audible during the systole, diastole or both. Backward regurgitation (due to a leaking valve, atrial or ventricular septal defect or arteriovenous connection), forward flow through narrowed or deformed valves, a high rate of blood through normal or abnormal valves, vibration of loose structures within the heart, or continuous flow through A-V shunts are some common causes of murmurs [7].

Spectral analysis and parametric modelling have been widely applied to heart sound analysis [2]-[5], [8]. Those methods, which are based on second-order statistics, did not take into account the nonlinearity and non Gaussianity of the analyzed signals, since the second-order statistics (autocorrelation) suppress any phase information. More recent works include the use of the S Transform [9], the generalized spectral coherence [10], the Wigner-Ville distribution [11]-[12], neural networks [13]-[15], wavelet transform [16]-[17], and wavelet packet decomposition [18], in order to reveal information about the non-stationarity of the analyzed signals. Additionally, higher-order statistics have been introduced [19]-[20], which preserve the phase characteristics of the signals, resulting in detection of their deviation from Gaussianity. However, no method has combined wavelet transform with higher-order statistics to examine both the non-stationarity and non-Gaussianity of murmurs.

In the current study, this combinatory approach is examined for the nonlinear analysis of murmurs, combining the wavelet transform with higher-order statistics, resulting in the so-called wavelet bispectrum and wavelet bicoherence [21].

The authors are with the Department of Electrical and Computer Engineering, Aristotle University of Thessaloniki, GR 54124 Thessaloniki, Greece (corresponding author S. Taplidou: Tel.: +30-2310-994180; FAX: +30-2310-996312; e-mail: stellata@auth.gr).

II. Methodology

A. Continuous Wavelet Transform (CWT)

The continuous wavelet transform (CWT) is defined as [22]

$$W_x(a,b) = \frac{1}{\sqrt{a}} \int_{-\infty}^{\infty} x(t)\psi^*\left(\frac{t-b}{a}\right)dt \,, \qquad (1)$$

where $x(t)$ is the signal in time-domain, ($x(t) \in L^2(\Re)$), * is the complex conjugate and $\psi(t)$ is the mother wavelet scaled by a factor a, $a > 0$, and dilated by a factor b. In the CWT, the time and scale parameters (a,b) are continuous. Due to its direct analogy to the Fourier transform, the complex Morlet wavelet is chosen for the realization of the CWT, which is given by [23]

$$\psi(t) = \frac{1}{\sqrt{\pi f_b}} e^{-t^2/f_b} e^{j2\pi f_c t} \,, \qquad (2)$$

where f_b is a bandwidth parameter and f_c is the wavelet center frequency.

B. Higher-Order Spectra (HOS)

The bispectrum (BS) $B(\omega_1, \omega_2)$ of a process $\{X(k)\}$ is defined as [24]:

$$B(\omega_1, \omega_2) = E\{X(\omega_1)X(\omega_2)X^*(\omega_1 + \omega_2)\} \,, \qquad (3)$$

where $E\{\cdot\}$ is the expectation value, $X(\omega_i), i = 1,2$ is the complex Fourier coefficient of the process $\{X(k)\}$ at frequencies ω_i and $X^*(\omega_i)$ is its complex conjugate. The bicoherence (BC), or normalized BS, is defined as [24]:

1-4244-0033-3/06/$20.00 ©2006 IEEE.

$$b(\omega_1,\omega_2)=\frac{B(\omega_1,\omega_2)}{[P(\omega_1)P(\omega_2)P(\omega_1+\omega_2)]^{1/2}}, \quad (4)$$

where $P(\omega_i), i=1,2$ is the power spectrum at frequencies ω_i of the process. The magnitude of BC, $|b(\omega_1,\omega_2)|$, or bicoherency index, constitutes a measure of the amount of quadrature phase-coupling that occurs in a signal between any two of its frequency components, due to their non-linear interactions. The bicoherence index is bounded between 0 and 1; when $|b(\omega_1,\omega_2)|$ is equal to 1, the frequency components at ω_1 and ω_2 are completely phase-coupled, whereas, when $|b(\omega_1,\omega_2)|$ is equal to 0, there is no quadrature phase-coupling between the harmonics at ω_1 and ω_2 [25].

C. Wavelet-based HOS

By analogy to the definition of the bispectrum in Fourier terms (see (3)), the wavelet bispectrum (WBS) is defined as [21]

$$B_w(a_1,a_2)=\int_T W_x^*(a,\tau)W_x(a_1,\tau)W_x(a_2,\tau)d\tau, \quad (5)$$

where the integration is done over a finite time interval $T:\tau_0\le\tau\le\tau_1$, and α,α_1,α_2 satisfy the following rule:

$$\frac{1}{a}=\frac{1}{a_1}+\frac{1}{a_2}. \quad (6)$$

WBS expresses the amount of quadrature phase-coupling in the interval T, which occurs between wavelet components of scale lengths $a_1, a_2,$ and a of $x(t)$ such that the sum rule of (6) is satisfied. By interpreting the scales as inverse frequencies, $\omega=2\pi/a$, the WBS can be interpreted as the coupling between wavelets of frequencies that satisfy $\omega=\omega_1+\omega_2$, within the frequency resolution.

Similarly to the definition of BC (see (4)), the wavelet bicoherence (WBC) can be defined as the normalized WBS, i.e.,

$$b_w(a_1,a_2)=\frac{B_w(a_1,a_2)}{\left\{\left[\int_T|W_x(a_1,\tau)W_x(a_2,\tau)|^2d\tau\right]\left[\int_T|W_x(a,\tau)|^2d\tau\right]\right\}^{1/2}} \quad (7)$$

which magnitude $|b_w(a_1,a_2)|$ can attain values between 0 and 1. For ease of interpretation, the squared WBC plotted in the $(\omega_1,\omega_2)-$plane, i.e., $|b_w(\omega_1,\omega_2)|^2$, is preferred. Due to the symmetries in the definition and the limitation set by the Nyquist frequency ω_s [26], the estimation of WBC in the whole bi-frequency plane can be based on its values in the principal region $\{\Delta:\omega_1,\omega_2\le\omega_1,\omega_1+\omega_2\le\omega_s\}$.

Since the WBC defined in (7) refers to a certain time interval T, its value is corresponded to the center of this interval, i.e., $t_0=T/2$. Consequently, the evolutionary WBC (EWBC) can be defined as

$$\mathbf{b}_w(\omega_1,\omega_2,t)=\{b_w(\omega_1,\omega_2)|_{t=t_0+k\Delta T_1}\},\quad k=0,1,2,3,...;(2\pi/\omega_s)\le\Delta T_1\wedge k\Delta T_1\le T_{total}-2t_0, \quad (10)$$

where T_{total} is the total time duration of the analyzed signal $x(t)$. When using EWBC, the evolution of the nonlinearities across time can be represented, within a time-resolution controlled by the selection of the ΔT_1 value. For a two-dimensional estimation of the variation of the wavelet bicoherence over time, the energy of the evolutionary wavelet bicoherence (EEWBC) is introduced, which is defined as

$$E_{b_w}(t)=\sum_T b_w^2(\omega_1,\omega_2) \quad (11)$$

In general, the numerical values of EEWBC depend on the chosen calculation grid, thus they provide qualitative summarization of the underlying information.

III. Data Set and Implementation Issues

The proposed analysis was tested on pre-classified heart sound signals appropriate for physicians' training, corresponding to abnormal heart sounds and heart murmurs, drawn from a heart sound database [27]. Sections of 15 s (containing 20 heart beats on average) of every signal were digitized with a 16-bit A/D converter at a sampling frequency of $f_s=11.025$ kHz. Records of 8000 samples were divided into 512-point segments, with an 80% overlapping percentage, and the wavelet bispectrum and wavelet bicoherence of each segment were estimated. Heart sound analysis was carried out using Matlab 7.0 (The Mathworks Inc., Natick, MA). The frequency range of analysis was selected as $f=10:10:400$ Hz with corresponding scales calculated by $a=f_cf_s/f$, a central frequency of complex Morlet wavelet at $f_c=0.8125$ Hz and its bandwidth parameter equal to $f_b=128$. The energy of the evolutionary wavelet bicoherence is estimated within the frequency range $f=130:10:400$ Hz, because the aim is to observe the effect of the murmurs' existence, which appear at frequencies higher than those of S_1 and S_2 sounds.

IV. Results and Discussion

Figure 1 depicts an 8000-point segment of a heart sound recording from a patient with aortic stenosis and aortic insufficiency. In Fig. 1(a) the normalized heart sound signal in the time domain is depicted. As it can be seen from Fig. 1(a), the recorded signal exhibits two high amplitude sections that correspond to heart sounds S1 and S2 (~0-0.05 s and ~0.3-0.35 s respectively) and a murmur between the two normal heart sounds (~0.05-0.3 s). Fig. 1(b) shows the corresponding energy of the evolutionary wavelet bicoherence for frequencies between 130 and 400 Hz. From this figure, it is apparent that the EEWBC exhibits a decrease when corresponding to the normal heart sounds (S1 and S2), i.e., the degree of the phase coupling of the frequency content at the frequency range under investigation is low. In Fig. 1(c), the

wavelet coefficients that correspond to a 512-point segment of the S1 heart sound (~0.02-0.06 s) are depicted. From this figure, the existence of one dominant low frequency is apparent. In Fig. 1(d), the corresponding squared wavelet bispectrum is depicted. The phase coupling that takes place is due to this only one frequency. In Fig. 1(e), the wavelet coefficients that correspond to a 512-point segment of the heart murmur (~0.06-0.10 s) are shown. From this figure, the presence of multiple higher frequencies is apparent. In Fig. 1(f), the corresponding squared wavelet bispectrum is depicted. Quadrature phase-coupling exists between the harmonics revealed in the wavelet bispectrum content corresponding to the heart murmur. In particular, the distinct peaks appear at $(f_1, f_2) \approx (100,100)$ Hz, $(f_1, f_2) \approx (100,200)$ Hz, and $(f_1, f_2) \approx (100,300)$ Hz. Self-phase coupling is also present at $(f_1, f_2) \approx (200,200)$ Hz, which is related to the frequency located at $f_3 = f_1 + f_2 \approx 400$ Hz.

The results from the analysis of another case are shown in Fig. 2. In particular, Fig. 2 depicts an 8000-point segment of a heart sound recording from a patient with patent ductus arteriosus. In Fig. 2(a) the normalized heart sound signal in the time domain is depicted. As it can be seen from this figure, the acquired signal exhibits two high amplitude sections that correspond to heart sounds S1 and S2 (~0-0.05 s and ~0.35-0.4 s respectively) and a murmur between the two normal heart sounds (~0.05-0.35 s). Fig. 2(b) shows the corresponding energy of the evolutionary wavelet bicoherence for frequencies between 130 and 400 Hz.

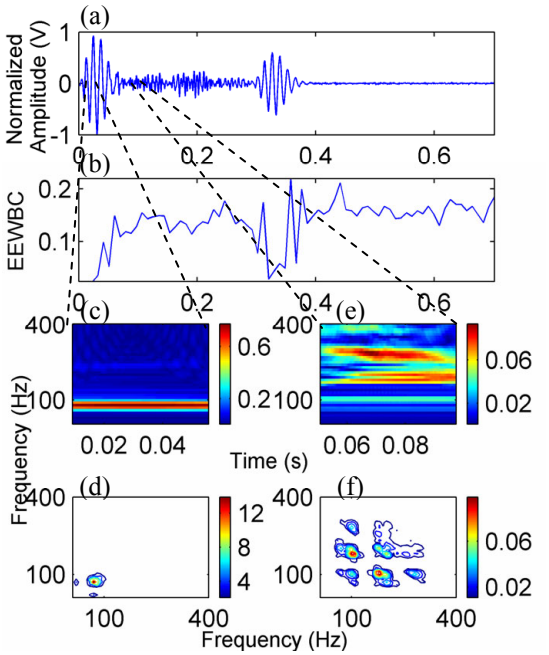

Fig. 1. An example of the analyzed signal that corresponds to a patient with aortic stenosis and aortic insufficiency. (a) An 8000-point segment of the signal under investigation; (b) energy of the evolutionary wavelet bicoherence; (c) wavelet coefficients of a 512-point segment of the heart sound S1; (d) corresponding WBS; (e) wavelet coefficients of a 512-point segment of the heart murmur; (f) corresponding WBS.

From this figure, it is apparent that, similarly to the previous examined case, the EEWBC exhibits a decrease when corresponding to the normal heart sounds, i.e. the degree of phase coupling of the frequency content at the frequency range under investigation is low. In Fig. 2(c), the wavelet coefficients that correspond to a 512-point segment of the S1 heart sound (~0.02-0.06 s) are depicted. The existence of one dominant low frequency is apparent here. In Fig. 2(d), the corresponding squared wavelet bispectrum is depicted. Again, the phase coupling that takes place is due to this only frequency. In Fig. 1(e), the wavelet coefficients that correspond to a 512-point segment of the heart murmur (~0.54-0.58 s) are shown. From this figure, the presence of multiple high frequencies is apparent. In Fig. 2(f), the corresponding squared WBS is depicted. Quadrature phase-coupling exists between the harmonics revealed in the wavelet bispectrum content corresponding to the heart murmur. In particular, the distinct peaks appear at $(f_1, f_2)_{p_1} \approx (75,125)$ Hz, $(f_1, f_2)_{p_2} \approx (75,150)$ Hz and $(f_1, f_2)_{p_3} \approx (75,250)$ Hz, which are related to frequencies $f_3 = (f_1 + f_2)_{p_1} \approx 200$ Hz, $f_4 = |f_1 - f_2|_{p_2} \approx 75$ Hz and $f_5 = |f_1 - f_2|_{p_3} \approx 175$ Hz, respectively. Self-phase coupling is also present at $(f_1, f_2) \approx (125,125)$ Hz, which is related to the frequency located at $f_6 = f_1 + f_2 \approx 250$ Hz ($p_i, i = 1,2,3,$ denotes the bi-frequency pairs). These results show that the wavelet-based higher-order spectral parameters capture the nonlinear characteristics of murmurs during the S1 to S2 transition.

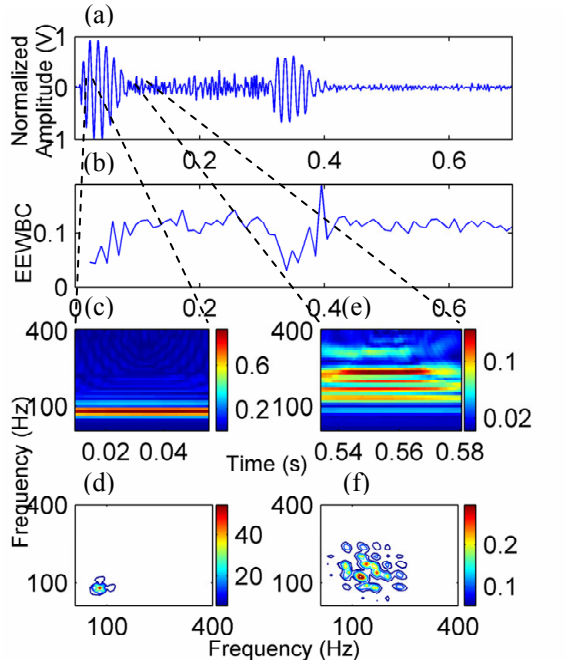

Fig. 2. An example of the analyzed signal that corresponds to a patient with patent ductus arteriosus. (a) An 8000-point segment of the signal under investigation; (b) energy of the evolutionary wavelet bicoherence; (c) wavelet coefficients of a 512-point segment of the heart sound S1; (d) corresponding WBS; (e) wavelet coefficients of a 512-point segment of the heart murmur; (f) corresponding WBS.

When comparing the results shown in Figs. 1 and 2, it can be seen that the difference in the pathology is reflected in the bi-frequency domain. In particular, a shifting is noticed between the main frequency pairs that exhibit quadrature phase coupling.

Moreover, in the case of patent ductus arteriosus, the wavelet bispectrum of the corresponding murmur (Fig. 2(f)) is more defused compared to the one from the murmur of aortic stenosis and aortic insufficiency (Fig. 1(f)). When observing both murmurs in the time domain, an increased similarity in their morphology is noticed, unlike the clear differences that they exhibit in the wavelet bispectrum domain. This shows the discrimination ability of the wavelet-based higher-order spectrum to differentiate between different pathologies with similar heart sound impression. To this end, the proposed analysis could be used as an advanced tool that could contribute to the objective analysis of pathological heart sounds, such as murmurs.

V. Conclusion

A combination of wavelet transform with third-order statistics/spectra applied to nonlinear analysis of heart sounds related to heart pathology was presented in the current study. This approach reveals the nonlinear characteristics of heart murmurs, as they evolve during the cardiac sound patter. The promising results presented here allow the extension of this analysis to large-scale experiments, to further explore the association of these nonlinear characteristics of heart sounds with the type and the severity of the related pathology.

References

[1] J. Semmlow, W. Welkowitz, J. Kostis, and J. W. Mackenzie, "Coronary artery disease-correlates between diastolic auditory characteristics and coronary artery stenoses," *IEEE Trans. Biomed. Eng.*, vol. 30, pp. 136-139, 1983.

[2] M. Akay, J. Semmlow, W. Welkowitz, M. Bauer, and J. Kostis, "Detection of coronary occlusions using AR modeling of diastolic heart sounds," *IEEE Tran. Biomed. Eng.*, vol. 37, pp. 366-373, 1990.

[3] P. D. Stein, H. N. Sabbah, J. B. Lakier, S. R. Kemp, and D. J. Magilligan, "Frequency spectra of the first heart sound and of the aortic component of the second heart sounds in patients with degenerated porcine bioprosthetic valves," *Amer. J. Cardiol.*, vol. 53, pp. 557-561, 1984.

[4] R. Beyer, S. Levkovitz, S. Braun, and Y. Polti, "Heart sounds processing by average and variance calculation-Physiologic basic and clinical implications," *IEEE Trans. Biomed. Eng.*, vol. 31, no. 9, pp. 591-596, Sept. 1984.

[5] L. G. Durand, J. De Guise, and R. Guardo, "FFT techniques for the spectral analysis of prosthetic heart valve sounds," in *4th Ann. Symp. Comp. Appl. Med. Care IEEE*, Washington, DC, 1980, pp. 1005-1011.

[6] M. Akay, J. Semmlow, W. Welkowitz, M. Bauer, and J. Kostis, "Noninvasive detection of coronary occlusions using eigenvector methods before and after angioplasty," *IEEE Trans. Biomed. Eng.*, vol. 37, no. 11, pp. 1095-1106, Nov. 1991.

[7] B. Erickson, Heart sounds and murmurs: a practical guide, 3rd ed., Mosby, St. Louis, Missouri, 1997.

[8] R. M. Rosen, B. S. Shakktottai, P. Parthasarathy, A. F. Turner, D. H. Blankenhorn, and E. J. Roshcke, "Phonoangiography by auto-correlation," *Circulation*, vol. 55, no. 4, pp. 626-633, 1977.

[9] G. Livanos, N. Ranganathan, and J. Jiang, "Heart sound analysis using the S Transform," *IEEE Comp. in Cardiol.*, vol. 27, pp. 587-590, 2000.

[10] N. L. Gerr and J. C. Allen, "The generalized spectrum and spectral coherence of a harmonizable time series," *Dig. Sign. Process.*, vol. 4, pp. 222-238, 1994.

[11] D. Einstein, K. S. Kunzelman, P. Reinhall, M. Tapia, R. Thomas, Ch. Rothnie, and R. P. Cochran, "Non-invasive determination of mitral valve acoustic properties: a proposed method to determine tissue alteration due to disease," *in Proc. of 1st Joint BMES/EMBS Conf. Serv. Human., Adv. Techn IEEE.*, Atlanta, GA, 1999, p. 183.

[12] Sh. Daliman and Ah. Z. Sha'ameri, "Time-frequency analysis of heart sounds using windowed and smooth windowed Wigner-Ville distribution," in *7th Intern. Symp. on Sign. Process. and its Appl.*, vol. 2, 2003, pp. 625-626.

[13] T. Oskiper and R. Wattrous, "Detection of the first heart sound using a time-delay neural network," *IEEE Comp. in Cardiol.*, vol. 29, pp. 537-540, 2002.

[14] Z. M. Zin, Sh. Hussain-Salleh, and M. D. Sulaiman, "Wavelet analysis and classification of mitral regurgitation and normal heart sounds based on artificial neural networks," in *7th Intern. Symp. on Sign. Process. and its Appl.*, 2003, pp. 619-620.

[15] R. Folland, E. L. Hines, P. Boilot, and D. Morgan, "Classifying coronary dysfunction using neural networks through cardiovascular auscultation," *Med. Biol. Eng. Comput.*, vol. 40, pp. 339-343, 2002.

[16] J. J. Lee, S. M. Lee, I. Y. Kim, H. K. Min, and S. H. Hong, "Comparison between Short Time Fourier and Wavelet Transform for feature extraction of heart sound," in *IEEE Reg. 10 Conf. TENCON*, 1999, pp. 1547-1550.

[17] O. Say, Z. Dokur, and T. Olmez, "Classification of heart sounds by using wavelet transform," *IEEE*, pp. 128-129, 2002.

[18] H. Liang and I. Hartimo, "A feature extraction algorithm based on wavelet packet decomposition for heart sound signals," in *IEEE-SP Intern. Symp. on Time-Frequency Time-Scale Anal.*, 1998, pp. 93-96.

[19] B. Ergen and Y. Tatar, "The analysis of heart sounds based on linear and high order statistical methods," in *23rd Ann. Intern. Conf. EMBS of IEEE,* vol. 13, 2001, pp. 2139-2141.

[20] L. J. Hadjileontiadis and S. M. Panas, "Discrimination of heart sounds using higher-order statistics," in *Proc. 19th Intern. Conf. IEEE/EMBS*, Chicago, IL, 1997, pp. 1138-1141.

[21] B. Ph. van Milligen, C. Hidalgo, and E. Sánchez, "Nonlinear phenomena and intermittency in plasma turbulence," *Phys. Rev. Letters*, vol. 74, no. 3, pp. 395-398, 1995.

[22] P. S. Addison, *The illustrated wavelet transform handbook: Introductory theory and applications in science, engineering, medicine and finance*, Bristol: Institute of Physics (IOP) Publishing, 2002.

[23] *Wavelet toolbox*, Matlab Version 7.0, The Mathworks, Inc., 2004.

[24] Ch. L. Nikias and A. M. Petropoulou, *Higher-order spectra analysis: a nonlinear signal processing framework*, New Jersey: PTR Prentice-Hall Inc., 1993.

[25] Ch. P. Ritz, E. J. Powers, and R. D. Bengston, "Experimental measurement of three-wave coupling and energy cascading," *Phys. Fluids B*, vol. 1, no. 1, pp. 153-163, 1989.

[26] Y. C. Kim and E. J. Powers, "Digital bispectral analysis of self-excited fluctuation spectra," *Phys. Fluids*, vol. 21, pp. 1452-1453, 1978.

[27] A. G. Tilikian and M. B. Conover, *Understanding heart sounds and murmurs with an introduction to lung sounds*, 3rd ed., W. B. Saunders Co., Philadelphia, Pa. 19106, workbook & tape, 1993.